Frataxin activates mitochondrial energy conversion and oxidative phosphorylation

Michael Ristow*†, Markus F. Pfister*, Andrew J. Yee*, Markus Schubert*, Laura Michael*, Chen-Yu Zhang‡, Kojhiro Ueki*, M. Dodson Michael II*, Bradford B. Lowell‡, and C. Ronald Kahn*†

*Joslin Diabetes Center, Harvard Medical School, Research Division, Boston, MA 02215; and ‡Beth Israel Deaconess Medical Center, Division of Endocrinology and Metabolism, Department of Medicine, Boston, MA 02215

Contributed by C. Ronald Kahn, August 22, 2000

Friedreich's ataxia (FA) is an autosomal recessive disease caused by decreased expression of the mitochondrial protein frataxin. The biological function of frataxin is unclear. The homologue of frataxin in yeast, *YFH1*, is required for cellular respiration and was suggested to regulate mitochondrial iron homeostasis. Patients suffering from FA exhibit decreased ATP production in skeletal muscle. We now demonstrate that overexpression of frataxin in mammalian cells causes a Ca^{2+}-induced up-regulation of tricarboxylic acid cycle flux and respiration, which, in turn, leads to an increased mitochondrial membrane potential ($\Delta\psi_m$) and results in an elevated cellular ATP content. Thus, frataxin appears to be a key activator of mitochondrial energy conversion and oxidative phosphorylation.

Friedreich's ataxia (FA) is a degenerative disease clinically characterized by progressive ataxia and hypertrophic cardiomyopathy leading to premature death (ref. 1; and http://www.ncbi.nlm.nih.gov/htbin-post/Omim/dispmim?229300). Patients also exhibit disturbances in glucose metabolism and, although frequently wheelchair bound, are of low body weight (2, 3). Additionally, patients with FA (4) as well as heterozygous relatives of FA patients (5) exhibit an early-onset insulin resistance. Furthermore, we and others have demonstrated decreased ATP production in postexercise skeletal muscle in FA patients (6, 7).

FA is caused by a deficiency of frataxin (8), a 210-aa nuclear-encoded mitochondrial protein highly conserved through evolution (9, 10). Frataxin is expressed in tissues with high metabolic activity, including brown fat, heart, liver, and certain neurons and neuroendocrine cells as found in the pancreas (9, 11). In FA, expression of frataxin is severely reduced (12) because of inhibition of the transcriptional machinery by expansion of an intronic GAA repeat (8, 13–16).

Frataxin is associated with mitochondrial membranes and appears to be involved in mitochondrial iron homeostasis. Deletion of the frataxin yeast homologue (YFH1) results in mutant strains that show a growth defect on fermentable carbon sources, accumulate mitochondrial iron, and exhibit a high sensitivity to oxidative stress induced by oxidant agents, as well as a reduction in mitochondrial respiration (9, 17–20).

The exact biochemical function of frataxin remains unclear. Although it has been suggested that frataxin might be an iron storage protein (21), recent data are challenging this view: (*i*) The targeted disruption of the mouse frataxin gene leads to early embryonic lethality, although no increase in iron accumulation could be observed (22). (*ii*) Restoration of YFH1 in a deficient yeast strain is unable to rescue the loss of aconitase (23), a mitochondrial enzyme typically reduced in FA (24). (*iii*) There is no evidence for an increased iron load in FA patients (25). (*iv*) The crystal structure of human frataxin does not provide evidence for any specificity in iron binding (26). (*v*) Deficiencies of proven mitochondrial iron transporters exhibit a phenotype clearly different from FA (http://www.ncbi.nlm.nih.gov/htbin-post/Omim/dispmim?301310), whereas patients suffering from isolated familial deficiency of vitamin E (α-tocopherol) leading to depletion of this exogenous antioxidant are clinically indistinguishable from FA (http://www.ncbi.nlm.nih.gov/htbin-post/Omim/dispmim?277460).

We therefore hypothesized that frataxin might primarily affect oxidative phosphorylation (OXPHOS) rather than regulate iron storage, since the latter is an ATP-dependent process. Here, we provide evidence that frataxin functions as an activator of OXPHOS, leading an increased mitochondrial membrane potential $\Delta\psi_m$ and an elevated cellular ATP content. This would explain the previous findings of deficits in cellular respiration in YFH1-deficient yeast. The results described herein provide a unifying model for the clinical and biochemical findings in FA.

Materials and Methods

Cell Culture. 3T3-L1 preadipocytes were obtained from American Type Culture Collection (lot no. F-15409) and cultured in DMEM with 4.5 g D-glucose/liter (BRL) and 10% heat inactivated bovine calf serum (HyClone). Transfected cells were maintained in media as above containing 2 mg/liter puromycin (Sigma). Differentiation was induced as described previously (27) by using media containing puromycin.

Constructs and Transfection. Human *frataxin* cDNA was cloned into *Bam*HI and *Eco*RI sites of pBluescript KS (Stratagene) after PCR amplification with specific primers carrying the appropriate restriction sites at their 5′ ends from reverse transcribed human heart mRNA (CLONTECH). After exclusion of PCR-induced random mutations by sequencing, the full-length cDNA was subcloned into *Bam*HI and *Eco*RI sites of pBabe-Puro, a retroviral expression plasmid (28), generating pBabe-Puro-*hFrataxin*. This construct was transfected into ecotrophic Phoenix producer cells, and the supernatant was used to infect 3T3-L1 cells, which were transferred into puromycin-containing media 48 h after initiation of infection. Control cells were generated similarly, except for the pBabePuro-*hFrataxin* was replaced by the original pBabePuro as a vehicle.

Northern blotting was done according to standard procedures (29) by using QuikHyb solution (Stratagene) and hybridization at 68°C with a mouse *frataxin* probe generated by PCR from the 3′ half of the cDNA (for Fig.1*a*) and an *aP2* probe (a kind gift of B. Spiegelman, Dana Farber Cancer Institute) for Fig. 1*e*. High stringency washes were performed at 45°C and 60°C, respectively. RNA samples were extracted from confluent tissue culture dishes by using Ultraspec (Biotecx Laboratories, Hous-

Abbreviations: FA, Friedreich's ataxia; YFH1, frataxin yeast homologue; OXPHOS, oxidative phosphorylation; PDH, pyruvate dehydrogenase; ICDH, isocitrate dehydrogenase; FCCP, carbonyl cyanide *p*-(tri-fluoromethoxy) phenylhydrazone; MSH buffer, 210 mM D-mannitol, 70 mM sucrose, and 5 mM K^+-Hepes, pH 7.4; TCA, tricarboxylic acid.

†To whom reprint requests should be addressed. E-mail: c.ronald.kahn@joslin.harvard.edu or michael.ristow@uni-koeln.de.

The publication costs of this article were defrayed in part by page charge payment. This article must therefore be hereby marked "*advertisement*" in accordance with 18 U.S.C. §1734 solely to indicate this fact.

Article published online before print: *Proc. Natl. Acad. Sci. USA*, 10.1073/pnas.220403797. Article and publication date are at www.pnas.org/cgi/doi/10.1073/pnas.220403797

ton), and 20 μg total RNA was loaded per lane. Integrity and amounts of RNA were confirmed by stripping and reprobing the blot with a *36B4*-probe (a kind gift of George King, Joslin Diabetes Center) for the *frataxin* blots (data not shown) or a *tubulin* probe for the *aP2*-blots in Fig.1*e*. It should be noted that the mouse *frataxin* probe preferentially detects mouse *frataxin* RNA, thus the intensity of the transgenic human *frataxin* RNA signal (Fig. 1*a*) does not depict proportional expression levels.

Oil Red O staining was performed to assess cellular triglyceride content (30).

Triglyceride quantification was performed by using the GPO trinder kit (Sigma). Briefly, sonicated cellular extracts containing triglycerides were treated with lipoprotein lipase generating glycerol, which was converted into glycerol-1-phosphate, which then was oxidized into dihydroxyacetone phosphate and hydrogen peroxide. The reduction of the latter was quantified photometrically at 540 nm.

Lipid synthesis assay was performed by quantifying conversion of radiolabeled ^{14}C-glucose into lipid soluble material (31).

Glucose transport assay was performed by using 100 nM insulin to stimulate uptake of tritiated 2-deoxy-glucose (32).

Glycogen synthesis assay was performed by hydrolyzation of free glucose and subsequent conversion of glycogen into glucose by amyloglucosidase (33). Glucose was then quantified microfluorometrically (34).

Lactate was quantified by using a colorimetric kit (Sigma) in which a lactate oxidase converts lactate into pyruvate, and hydrogen peroxide, which was then quantified as above. Lactate content of tissue culture media was performed by using phenol-red free solutions (BRL).

Pyruvate dehydrogenase (PDH) was quantified by a standard spectrophotometric method that measures formation of NADH at 340 nm in the presence of 2.5 mM NAD, 0.3 mM thiamin pyrophosphate, 0.1 mM CoA, 0.3 mM DTT, 5 mM pyruvate, 1 mM $MgCl_2$, 5 mM 2-mercaptoethanol, 0.5 mM K^+-EDTA and 0.2% (wt/vol) Triton X-100 as previously described (35).

Isocitrate dehydrogenase (ICDH) was quantified using a kinetic kit (Sigma) by mixing L-isocitrate and NADP in the presence of excess Mn^{2+}, where NADP is converted into NADPH, which is photometrically quantified per time at 340 nm.

Mitochondrial respiration was quantified by transferring manually detached cells into a 1-ml Clark-type oxygen electrode chamber at 37°C (36). After recording the basal respiration, maximal uncoupling was induced by adding carbonyl cyanide *p*-(tri-fluoromethoxy) phenylhydrazone (FCCP) (Sigma) in a final concentration of 2 μM (37).

Glucose oxidation assay was performed as described (38), except that hydroxylamine was replaced by KOH for capturing radiolabeled $^{14}CO_2$.

Cellular ATP was quantified by using a luciferase-based kit for cellular extracts (Sigma).

Southern blotting (29) was performed by using a probe for the mitochondrially encoded gene *cytochrome c* oxidase subunit II (a kind gift of Zhidan Wu, Dana Farber Cancer Institute), and the high stringency wash was done at 55°C. DNA samples were extracted from confluent dished by proteinase K digestion and subsequent precipitation in 2-propanol. Precipitates were redissolved in 1× restriction buffer appropriate for the endonuclease *Pst*I (Roche Molecular Biochemicals) and subjected to *Pst*I-digest overnight. Loading was 10 μg DNA per lane, which was confirmed by optical density and computerized comparison of ethidium bromide-stained 0.9% agarose gels.

Isolation of mitochondria was performed by dounce homogenization of cells and a subsequent differential centrifugation method (39). Mitochondrial pellets were washed twice in a buffer containing 210 mM D-mannitol, 70 mM sucrose, and 5 mM K^+-Hepes, pH 7.4 (MSH buffer). The final pellet was resuspended in MSH buffer and kept on ice for further experiments.

$^{45}Ca^{2+}$-uptake of isolated mitochondria was monitored by the radioisotope technique (40). Briefly, mitochondria (0.5 mg/ml) were incubated at 25°C in 1 ml of MSH buffer (as above) with continuous stirring. A total of 5 μM rotenone (Sigma) and 2.5 mM potassium succinate (prepared from succinic acid and KOH; both from Sigma) were subsequently added to energize the mitochondria. Where indicated, ruthenium red (Sigma), a specific inhibitor of mitochondrial Ca^{2+}-uptake (41), was added (final concentration: 2 nmol/mg mitochondrial protein). One minute after addition of rotenone and succinate, Ca^{2+}-uptake was initiated by addition of 200 μM Ca^{2+} with $^{45}Ca^{2+}$ (2000 dpm/nmol) as tracer. To induce Ca^{2+}-efflux, 5 mM EGTA (Sigma) was added 5 min after addition of Ca^{2+} (42). At the required times, 50-μl aliquots were withdrawn, vacuum filtered through Millipore filters (0.45 μm pore size), and rinsed twice with 1 ml of cold MSH buffer (as above). The radioactivity remaining on the filters was determined in a liquid scintillation counter.

Mitochondrial membrane potential was measured by rhodamine 123 (Sigma) staining performed in the tissue culture media for 10 min at a final concentration of 10 μg/liter at 37°C. Cells were then washed twice for 2 min each with phenol red-free media and subjected to digital fluorescence microscopy (Zeiss Axioinvert AXS100TV) at 488 nm excitation wavelength. Quantification of fluorescence was performed by using a software package openlab v2.0, based on three independent slides for each cell line evaluating three areas of each slide.

Protein content was measured photometrically by using the Bradford method (43).

Statistical analyses were performed by using SPSS for Windows, release 9.0.0, applying independent *t* tests assuming unequal variances. Differences were considered significant whenever $P < 0.05$. Error bars are depicted as plus two standard error means (+2 SEM).

Results and Discussion

Overexpression of Frataxin Increases Triglyceride Synthesis. We have created a 3T3-L1 adipocyte model (44) overexpressing human frataxin by means of retroviral transduction (Fig. 1*a*). When these cells were differentiated into adipocytes by using a standardized protocol (27), they accumulated triglyceride in a time-dependent manner (Fig. 1*b*). By the time of full differentiation at day 9, cells constitutively overexpressing frataxin accumulated 1.8 times more triglyceride ($P = 0.015$) (Fig. 1*c*). To confirm this observation by an independent method, the rate of triglyceride synthesis from ^{14}C-labeled glucose in the media was quantified (Fig. 1*d*). This assay revealed a parallel increase in ^{14}C-labeled organic soluble material in those cells overexpressing frataxin ($P = 0.032$). Northern blot analysis for *aP2* mRNA, a marker of terminal adipocyte differentiation, demonstrated a 2.2-fold increase when normalized for total RNA (Fig.1 *e* and *f*), consistent with the increased triglyceride accumulation as described above. These observations may be explained by an increase in energy conversion as well as by an activation of the cellular differentiation machinery (as indicated by Fig. 1*e*).

Frataxin Regulates Krebs Cycle Activity. To investigate whether frataxin leads to an increase in fat storage in adipocytes by causing an increase in uptake of energy or a more efficient conversion of glucose into lipid, we determined the flux of glucose and its tricarbon metabolites in this system. Cells overexpressing frataxin demonstrate a 1.5-fold increase of the uptake of nonmetabolizable 2-deoxy-glucose, both in the presence and absence of insulin ($P = 0.044$ and 0.028, respectively) (Fig. 2*a*). Although the storage of glycogen in these cells was unchanged (data not shown), lactate accumulation, an end-point

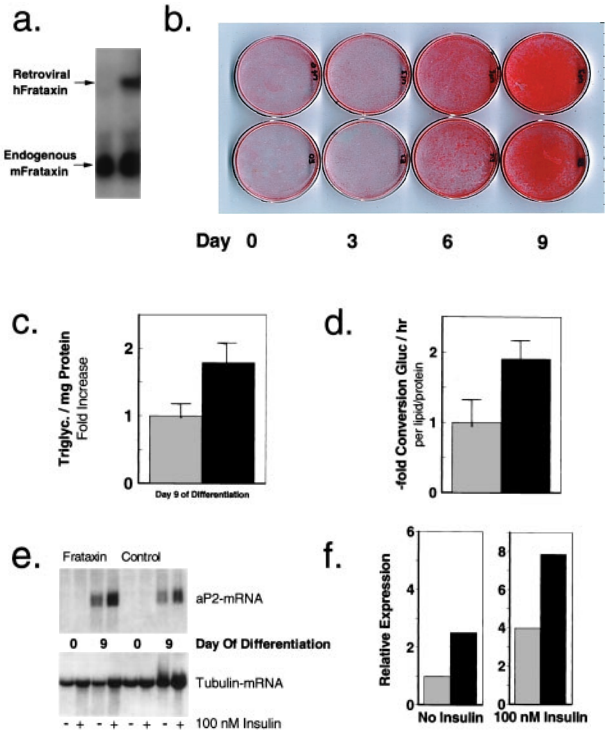

Fig. 1. Overexpression of frataxin promotes energy storage in adipocytes. (*a*) A Northern blot of total RNA from 3T3-L1 fibroblasts retrovirally transfected with vehicle (empty pBabe Puro, left lane) and human *frataxin* (right lane). The blot was probed with a 3′ fragment of a mouse *frataxin* cDNA. The human *frataxin* RNA migrates above the endogenous mouse *frataxin* RNA because of retroviral sequences flanking the transgenic human *frataxin*. (*b*) 3T3-L1-cells overexpressing human frataxin (upper row) compared with cells carrying the empty vector (lower row) during differentiation from fibroblasts (day 0, outer left column) to adipocytes (day 9, outer right column). Cells were formalin-fixed on the culture dish and stained with Oil Red O, a fat specific dye. (*c*) A quantification of triglyceride content in differentiated 3T3-L1 adipocytes (derived from *b*) using the GPO trinder method. The light bars represent cells transfected with the vehicle (100% equals 291 ± 22.9 μg/mg protein), the dark bars reflect cells overexpressing transgenic human frataxin. (*d*) The kinetic rate of triglyceride synthesis in cells overexpressing frataxin (dark bars) compared with control cells (light bars). The rate in control cells (100%) was 0.31 ± 0.067 nmol/h/organic soluble material/mg protein. (*e*) A Northern blot of total RNA extracted from 3T3L1 fibroblasts (day 0 of differentiation) and adipocytes (day 9 of differentiation) overexpressing human frataxin (left lanes) or empty vehicle (right lanes). The blot was first probed for *aP2*, a downstream regulator in late adipocyte differentiation, then stripped and reprobed with a *tubulin* probe to estimate the amount of RNA loaded. (*f*) The quantification of the signals from *e* by using IMAGEQUANT software. The light bars represent cells transfected with the vehicle, the dark bars reflect cells overexpressing human frataxin. The left pair of bars compares the amount of RNA in serum-starved cells, whereas the right pair was derived from cells stimulated with insulin at a concentration of 100 nM over a time period of 8 h.

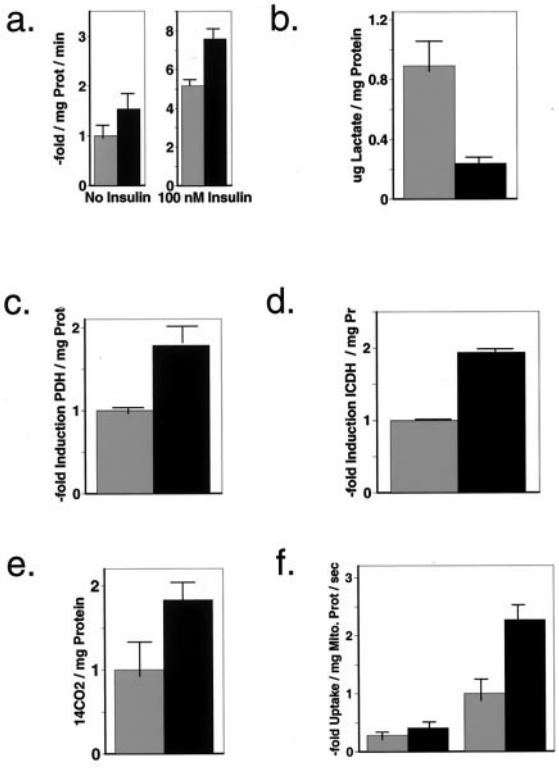

Fig. 2. Frataxin induces oxidative glucose metabolism by elevating mitochondrial calcium content. (*a*) Results of glucose transport assays performed with 3T3-L1-adipocytes expressing vehicle (light bars) or human frataxin (dark bars). Uptake of ^{3}H-labeled 2-deoxy-glucose was measured by scintillation counting in the absence (left pair) and in the presence of insulin (100 nM, 60 min, right pair). The radioactivity in the cell lysates is proportional to the amount of glucose taken up normalized for protein content (100% equals 0.60 ± 0.08 nmol/min/mg protein). (*b*) Measurement of lactate within cell lysates normalized for protein content. The amount of this tricarbon intermediate and end product of anaerobic glycolysis is depicted in light bars for the vehicle transfected cells (0.89 ± 0.082 μg/mg protein) and dark bars for frataxin overexpressing cells. (*c*) Photometric quantification of pyruvate dehydrogenase activity in control cells (light bars) and frataxin overexpressing cells (dark bars) normalized for protein content, indicating an increased acetyl-CoA synthesis. (*d*) Activity of isocitrate dehydrogenase normalized for protein content in an set of cells identical to the above, indicating an up-regulated TCA cycle activity. (*e*) Production of radiolabeled $^{14}CO_2$ subsequent to supplementing the cells with ^{14}C-glucose, reflecting increased glucose oxidation. (*f*) Uptake of $^{45}Ca^{2+}$ into isolated mitochondria in presence (left pair of bars) and absence (right pair of bars, light bar represents control [100%], which equals 0.026 ± 0.004 amol/mg mitochondrial protein/s) of ruthenium red, a specific blocker of the mitochondrial Ca^{2+} uniporter.

of anaerobic glycolysis, was decreased by 75% in cell lysates (P = 0.002) (Fig. 2*b*) and in the tissue culture media (data not shown) of the cells overexpressing frataxin. The decreased lactate levels together with increased glucose uptake and normal glycogen content indicate an elevated pyruvate metabolism. The rate-limiting step in pyruvate conversion is activity of the PDH complex. Previous studies have suggested that PDH activity is reduced in FA patients (48). Conversely, the activity of PDH was increased 1.7-fold in cells overexpressing frataxin (P = 0.002) (Fig. 2*c*), consistent with an increase in acetyl-CoA in these cells.

Acetyl-CoA is normally metabolized in the tricarboxylic acid (TCA) cycle, but is shuttled into the cytosol to be metabolized into triglycerides when synthesized in amounts exceeding the capacity of the TCA cycle (consistent with the results in Fig. 1). Therefore, we hypothesized that TCA cycle activity was maximized in the frataxin overexpressing cells. This hypothesis is supported by the finding that the activity of ICDH was up-regulated 1.8-fold (P = 0.001) (Fig. 2*d*). This is consistent with previous reports (45) suggesting decreased activity of another TCA cycle enzyme, 2-ketoglurate dehydrogenase, in tissues of FA patients. Furthermore, when cells were grown in media containing radioactively labeled ^{14}C-glucose, frataxin overexpressing cells showed a 1.8-fold increase in $^{14}CO_2$ release compared with control cells (P = 0.027), also indicating an increased TCA cycle activity (Fig. 2*e*).

Frataxin Increases Mitochondrial Ca^{2+} Uptake. One potential common denominator that might account for activation of PDH and ICDH would be an elevation in mitochondrial Ca^{2+} content

since both of these enzymes, as well as the mitochondrial dehydrogenases, are activated by Ca^{2+} (46). To test this hypothesis in viable mitochondria, we measured calcium transport into isolated mitochondria as previously described (47). Dynamic $^{45}Ca^{2+}$-uptake was increased by 2.2-fold ($P < 0.001$) (Fig. 2*f*, right pair of bars), an effect which could be blocked by preincubation with ruthenium red (Fig. 2*f*, left pair of bars), a specific blocker of the mitochondrial calcium uniporter. Furthermore, the specific uptake could be reversed by using the Ca^{2+}-chelator EGTA (data not shown). Thus, overexpression of frataxin elevates mitochondrial Ca^{2+} content potentially leading to increased TCA cycle activity as described above (Fig. 2 *c–e*). This elevated Ca^{2+} content might additionally indicate an increase in mitochondrial membrane potential ($\Delta\psi_m$) because Ca^{2+}-transport into mitochondria is a secondary process driven by electrochemical forces (48).

Frataxin Activates Mitochondrial Respiration in Mammalian Cells. Previous studies in yeast suggest a decrease in mitochondrial respiration following inactivation of the frataxin homologue *YFH1* (9, 18). To confirm these findings in a reciprocal model, we quantified mitochondrial respiration in the 3T3-L1 cells overexpressing frataxin. Indeed, oxygen consumption was increased by more than 2-fold in cells overexpressing frataxin when compared with control cells ($P = 0.018$) (Fig. 3 *a* and *b*, left pair of bars). These data are consistent with the above-mentioned observations in yeast. To determine whether this increase in respiration in our mammalian model could be explained by an elevated mitochondrial capacity, mitochondrial respiration was uncoupled in the cells by treatment with FCCP. Interestingly, oxygen uptake was significantly increased in cells overexpressing frataxin compared with control cells following this treatment ($P = 0.022$) (Fig. 3 *a* and *b*, right pair of bars), suggesting increased electron transport activity in the cells overexpressing frataxin.

Frataxin Elevates the Mitochondrial Membrane Potential. Increased cellular respiration indicates an activated electron transport chain within the inner mitochondrial membrane, suggesting the presence of an elevated mitochondrial membrane potential ($\Delta\psi_m$) in cells overexpressing frataxin. Although the biochemical function of frataxin is widely unknown, the protein has been demonstrated to be associated with mitochondrial membranes (9). To evaluate whether $\Delta\psi_m$ is increased in cells overexpressing frataxin, we stained the cells with the fluorescent rhodamine 123, a dye whose accumulation in mitochondria is directly proportional to $\Delta\psi_m$ (49). Rhodamine-stained cells overexpressing frataxin showed a increased fluorescence of mitochondria when compared with control cells (Fig. 3*c*). On computerized quantitation, the intensity was increased 2.5-fold in cells overexpressing frataxin, indicating an elevated $\Delta\psi_m$ ($P = 0.001$) (Fig. 3*d*).

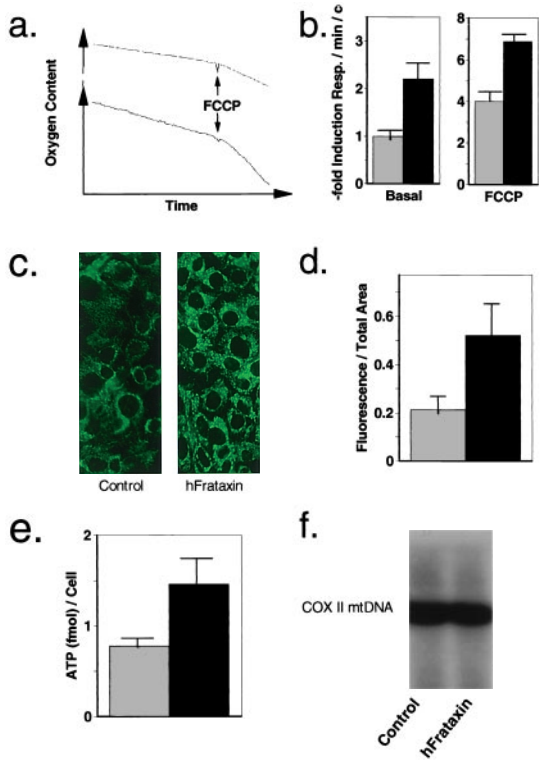

Fig. 3. Frataxin increases OXPHOS. (*a*) A typical signal recorded from the oxygen electrode chamber to measure cellular respiration. The upper graph reflects uptake of the control cells, whereas the lower graph was recorded by using frataxin overexpressing cells. (*b*) The calculated mitochondrial respiration in adipocytes overexpressing human frataxin (dark bars) or cells transfected with the empty vector (light bars) based on the slopes of the graphs in *a*. The left pair reflects basal oxygen consumption in these cells (100% equals 1.60 ± 0.11 nmol/min/10^6 cells), indicating increased respiration in cells overexpressing frataxin. The right pair reflects consumption after uncoupling with FCCP, thus reflecting an increased maximal mitochondrial capacity in the frataxin overexpressing cells. (*c*) A microphotograph (original enlargement 60-fold) of rhodamine 123-stained cells overexpressing frataxin (right) and mock-transfected cells (left), depicting increased fluorescence in overexpressing cells, indicating an elevated mitochondrial membrane potential. (*d*) Computerized quantification of rhodamine 123 fluorescence in cells overexpressing human *frataxin* (dark bars) or cells transfected with the empty vector (light bars). (*e*) Luciferase-based quantification of cellular ATP content in cells overexpressing human *frataxin* (dark bars) or cells transfected with the empty vector (light bars), indicating increased OXPHOS. (*f*) A Southern blot of total DNA (10 μg per lane) extracted from differentiated 3T3-L1-adipocytes expressing the empty vector (left lane) or human frataxin (right lane) using a probe for *cytochrome c* oxidase subunit II, the latter is exclusively encoded in the mitochondrial DNA and thus reflects the amount of mitochondrial DNA relative to total DNA loaded.

Frataxin Activates OXPHOS. We and others have described decreased ATP production in postexercise skeletal muscle in FA patients (6, 7). The reasons for this observation are unknown. The findings of an elevated $\Delta\psi_m$ in cells overexpressing frataxin might provide an explanation for the observations in humans.

Because $\Delta\psi_m$ is known to be the driving force of ATP-synthesis by the enzyme F_1F_O-ATPase, and $\Delta\psi_m$ appears to be elevated subsequent to overexpression of frataxin, we hypothesized that this might lead to an increase in ATP content. Indeed, spectrophotometric quantitation of cellular ATP content revealed a 1.9-fold increase ($P = 0.015$) (Fig. 3*e*). To exclude that the elevation in mitochondrial capacity and in OXPHOS of frataxin overexpressing cells could be explained by an increased number of mitochondria, we quantified the relative number of these organelles by using Southern blotting for *cytochrome c* oxidase subunit II, a gene exclusively encoded in the mitochondrial DNA (Fig. 3*f*). This approach showed no difference in the amount of mitochondria, an observation consistent with previously published data obtained in muscle extracts from FA patients (45). Furthermore, Western blot analysis of cytochrome *c* content in the mitochondrial fractions of both cell lines indicated no difference in mitochondrial biogenesis (data not shown).

Taken together, the data suggest that frataxin is an activator of OXPHOS in eukaryotic cells. Because the identification of frataxin as the site of genetic basis for FA, considerable effort has been made to explain the molecular pathogenesis of this disorder. Previous data obtained in a yeast knock-out model for the frataxin homologue *YFH1* suggest a respiratory deficit (9, 17, 18). This leads to a growth-deficient or *petite*-phenotype in the

yeast (50). The present finding that frataxin is an activator of OXPHOS in mammalian cells suggests that a deficiency of frataxin in tissues of patients with FA would lead to a defective OXPHOS. This view is supported by the recently published findings that the FA-phenotype in humans is associated with reduced ATP-levels in skeletal muscle during exercise (6, 7). Additionally, a coenzyme Q derivate, idebenone, has been shown to ameliorate cardiac dysfunction in FA (51). This clinical observation is consistent with our findings that overexpression of frataxin results in an increased $\Delta\psi_m$ because a similar increase of $\Delta\psi_m$ is found following coenzyme Q10 treatment of hepatocytes, which also protects the cells from oxidative stress (52). Lastly, FA appears to be clinically indistinguishable from inherited α-tocopherol (vitamin E) deficiency (http://www.ncbi.nlm.nih.gov/htbin-post/Omim/dispmim?277460), suggesting a close phenotypic relationship between a diminished antioxidant defense (i.e., vitamin E deficiency) and a decrease in $\Delta\psi_m$ in FA as would be predicted by the present study, and as observed in cultured fibroblasts derived from FA patients (M.R., M.S., M.F.P., and C.R.K., unpublished observations). Conversely, frataxin might regulate mitochondrial iron efflux (20) indirectly by activation of the ATP-dependent iron-transporters *ATM1* in yeast (53) and *ABC7* in humans (54), respectively. This would suggest that regulation of OXPHOS by frataxin is the primary effect and leads to secondary alterations in mitochondrial iron homeostasis commonly believed to be the cause of FA.

In summary, our data indicate that frataxin activates OXPHOS and energy conversion and suggest that reduced levels of frataxin in FA patients primarily result in a disease of ATP deficiency rather than an alteration in mitochondrial iron metabolism. This might explain why tissues exclusively dependent on oxidative metabolism, i.e., neuronal and heart tissues (55), are most severely affected in patients with FA (ref. 1; and http://www.ncbi.nlm.nih.gov/htbin-post/Omim/dispmim?229300). These findings might additionally explain the metabolic disturbances associated with FA, such as diabetes mellitus and insulin resistance. Clearly, further studies will be needed to investigate implications for both cell biology and disease.

We thank Christoph Richter for helpful comments, Bruce M. Spiegelman and members of his lab for the *aP2*- and *COXII*-probes, and Morris F. White for the use of his digital microscope. M.R. was supported by Köln Fortune Grants 88/97 and 88/97V of the University of Cologne. M.F.P. was supported by a Swiss National Science Foundation Fellowship. A.J.Y. was a Howard Hughes Medical Institute Medical Student Research Training Fellow. This work is supported by National Institutes of Health Grant DK 45935 (to C.R.K.).

1. Friedreich, N. (1863) *Virchows Arch. Pathol. Anat. Physiol. Klin. Med.* **26,** 391–419.
2. Finocchiaro, G., Baio, G., Micossi, P., Pozza, G. & di Donato, S. (1988) *Neurology* **38,** 1292–1296.
3. Tolis, G., Mehta, A., Andermann, E., Harvey, C. & Barbeau, A. (1980) *Can. J. Neurol. Sci.* **7,** 397–400.
4. Khan, R. J., Andermann, E. & Fantus, I. G. (1986) *Metabolism* **35,** 1017–1023.
5. Hebinck, J., Hardt, C., Schoels, L., Vorgerd, M., Briedigkeit, L., Kahn, C. R. & Ristow, M. (2000) *Diabetes* **49,** 1604–1607.
6. Lodi, R., Cooper, J. M., Bradley, J. L., Manners, D., Styles, P., Taylor, D. J. & Schapira, A. H. (1999) *Proc. Natl. Acad. Sci. USA* **96,** 11492–11495.
7. Vorgerd, M., Schöls, L., Hardt, C., Ristow, M., Epplen, J. T. & Zange, J. (2000) *Neuromusc. Dis.* **10,** 430–435.
8. Campuzano, V., Montermini, L., Molto, M. D., Pianese, L., Cossee, M., Cavalcanti, F., Monros, E., Rodius, F., Duclos, F., Monticelli, A., *et al.* (1996) *Science* **271,** 1423–1427.
9. Koutnikova, H., Campuzano, V., Foury, F., Dolle, P., Cazzalini, O. & Koenig, M. (1997) *Nat. Genet.* **16,** 345–351.
10. Gibson, T. J., Koonin, E. V., Musco, G., Pastore, A. & Bork, P. (1996) *Trends Neurosci.* **19,** 465–468.
11. Jiralerspong, S., Liu, Y., Montermini, L., Stifani, S. & Pandolfo, M. (1997) *Neurobiol. Dis.* **4,** 103–113.
12. Campuzano, V., Montermini, L., Lutz, Y., Cova, L., Hindelang, C., Jiralerspong, S., Trottier, Y., Kish, S. J., Faucheux, B., Trouillas, P., *et al.* (1997) *Hum. Mol. Genet.* **6,** 1771–1780.
13. Bidichandani, S. I., Ashizawa, T. & Patel, P. I. (1998) *Am. J. Hum. Genet.* **62,** 111–121.
14. Mäueler, W., Kyas, A., Keyl, H. G. & Epplen, J. T. (1998) *Gene* **215,** 389–403.
15. Ohshima, K., Montermini, L., Wells, R. D. & Pandolfo, M. (1998) *J. Biol. Chem.* **273,** 14588–14595.
16. Sakamoto, N., Chastain, P. D., Parniewski, P., Ohshima, K., Pandolfo, M., Griffith, J. D. & Wells, R. D. (1999) *Mol. Cell.* **3,** 465–475.
17. Babcock, M., de Silva, D., Oaks, R., Davis-Kaplan, S., Jiralerspong, S., Montermini, L., Pandolfo, M. & Kaplan, J. (1997) *Science* **276,** 1709–1712.
18. Wilson, R. B. & Roof, D. M. (1997) *Nat. Genet.* **16,** 352–357.
19. Foury, F. & Cazzalini, O. (1997) *FEBS Lett.* **411,** 373–377.
20. Radisky, D. C., Babcock, M. C. & Kaplan, J. (1999) *J. Biol. Chem.* **274,** 4497–4499.
21. Isaya, G., Adamec, J., Rusnak, F., Owen, W. G., Naylor, S. & Benson, L. M. (1999) *Am. J. Hum. Genet.* **65,** Suppl., A167.
22. Cossee, M., Puccio, H., Gansmuller, A., Koutnikova, H., Dierich, A., LeMeur, M., Fischbeck, K., Dolle, P. & Koenig, M. (2000) *Hum. Mol. Genet.* **9,** 1219–1226.
23. Foury, F. (1999) *FEBS Lett.* **456,** 281–284.
24. Rötig, A., de Lonlay, P., Chretien, D., Foury, F., Koenig, M., Sidi, D., Munnich, A. & Rustin, P. (1997) *Nat. Genet.* **17,** 215–217.
25. Wilson, R. B., Lynch, D. R. & Fischbeck, K. H. (1998) *Ann. Neurol.* **44,** 132–134.
26. Dhe-Paganon, S., Shigeta, R., Chi, Y. I., Ristow, M. & Shoelson, S. E. (2000) *J. Biol. Chem.*, in press.
27. Student, A. K., Hsu, R. Y. & Lane, M. D. (1980) *J. Biol. Chem.* **255,** 4745–4750.
28. Morgenstern, J. P. & Land, H. (1990) *Nucleic Acids Res.* **18,** 3587–3596.
29. Ausubel, F. M., Brent, R., Kingston, R. E., Moore, D. D., Seidman, J. G., Smith, J. A. & Struhl, K. (1997) *Short Protocols in Molecular Biology* (Wiley, New York).
30. Preece, A. (1972) *Manual for Histologic Technicians* (Little, Brown, Boston).
31. Tozzo, E., Shepherd, P. R., Gnudi, L. & Kahn, B. B. (1995) *Am. J. Physiol.* **268,** E956—E964.
32. Moyers, J. S., Bilan, P. J., Reynet, C. & Kahn, C. R. (1996) *J. Biol. Chem.* **271,** 23111–23116.
33. Patti, M. E., Virkamaki, A., Landaker, E. J., Kahn, C. R. & Yki-Jarvinen, H. (1999) *Diabetes* **48,** 1562–1571.
34. Passonneau, J. V. & Lowry, O. H. (1993) *Enzymatic Analysis: A Practical Guide* (Humana, Totowa, NJ).
35. Hinman, L. M. & Blass, J. P. (1981) *J. Biol. Chem.* **256,** 6583–6586.
36. Wu, Z., Puigserver, P., Andersson, U., Zhang, C. Y., Adelmant, G., Mootha, V., Troy, A., Cinti, S., Lowell, B. B., Scarpulla, R. C. & Spiegleman, B. M. (1999) *Cell* **98,** 115–124.
37. Heytler, P. G. (1979) *Methods Enzymol.* **55,** 462–442.
38. Gorus, F. K., Malaisse, W. J. & Pipeleers, D. G. (1984) *J. Biol. Chem.* **259,** 1196–1200.
39. Richter, C. (1984) *Methods Enzymol.* **105,** 435–441.
40. Lötscher, H. R., Winterhalter, K. H., Carafoli, E. & Richter, C. (1980) *J. Biol. Chem.* **255,** 9325–9330.
41. Saris, N. E. & Allshire, A. (1989) *Methods Enzymol.* **174,** 68–85.
42. Richter, C., Schweizer, M. & Ghafourifar, P. (1999) *Methods Enzymol.* **301,** 381–393.
43. Bradford, M. M. (1976) *Anal. Biochem.* **72,** 248–254.
44. Green, H. & Kehinde, O. (1974) *Cell* **1,** 113–116.
45. Blass, J. P., Kark, R. A. & Menon, N. K. (1976) *N. Engl. J. Med.* **295,** 62–67.
46. Gunter, T. E., Gunter, K. K., Sheu, S. S. & Gavin, C. E. (1994) *Am. J. Physiol.* **267,** C313—C339.
47. Crompton, M. & Carafoli, E. (1979) *Methods Enzymol.* **56,** 338–352.
48. Babcock, D. F. & Hille, B. (1998) *Curr. Opin. Neurobiol.* **8,** 398–404.
49. Chen, L. B. (1988) *Annu. Rev. Cell Biol.* **4,** 155–181.
50. Gray, J. V. & Johnson, K. J. (1997) *Nat. Genet.* **16,** 323–325.
51. Rustin, P., von Kleist-Retzow, J. C., Chantrel-Groussard, K., Sidi, D., Munnich, A. & Rötig, A. (1999) *Lancet* **354,** 477–479.
52. Teranishi, M., Karbowski, M., Kurono, C., Nishizawa, Y., Usukura, J., Soji, T. & Wakabayashi, T. (1999) *Arch. Biochem. Biophys.* **366,** 157–167.
53. Kispal, G., Csere, P., Guiard, B. & Lill, R. (1997) *FEBS Lett.* **418,** 346–350.
54. Allikmets, R., Raskind, W. H., Hutchinson, A., Schueck, N. D., Dean, M. & Koeller, D. M. (1999) *Hum. Mol. Genet.* **8,** 743–749.
55. Harding, A. E., Holt, I. J., Cooper, J. M., Schapira, A. H., Sweeney, M., Clark, J. B. & Morgan-Hughes, J. A. (1990) *Biochem. Soc. Trans.* **18,** 519–522.